3P3-7

Full-epitaxial ScAlN and MgZnO SMR based on epitaxial acoustic Bragg reflector

Satoshi Tokai[1,2†] and Takahiko Yanagitani[1,2,3,4*]
([1]Waseda Univ.; [2]ZAIKEN; [3]JST-CREST; [4]JST-FOREST)

1. Introduction

High sharpness (Q factors) is required for BAW filters to prevent interference between neighboring frequency bands. Lower dielectric and mechanical losses in the single crystalline piezoelectric thin films should contribute the increase of Q factors. Fabrication methods for single crystalline piezoelectric thin films are either the bulk crystal slicing technique of $LiNbO_3$ and $LiTaO_3$[1–6)] or epitaxial growth technique. Epitaxial growth technique might be better in order to obtain thin single crystalline layer in large areas of over 8 inches.

SMR[7)] consists of a piezoelectric thin film on acoustic Bragg reflector based on high and low impedance layers. However, to fabricate SMR with epitaxial piezoelectric layer, usual bottom-up process is difficult to be employed due to the amorphous SiO_2 in a low acoustic impedance layer.

In this study, we report SMR with epitaxial ScAlN or MgZnO piezoelectric layer based on epitaxial acoustic Bragg reflector.

2. Fabrication of full-epitaxial SMR

All epitaxial thin films were grown by RF magnetron sputtering. First, the acoustic Bragg reflector based on 5 pairs of epitaxial (0001) Ti / (111) Pt or 6 pairs of epitaxial (0001) ZnO / (111) Pt was grown on (0001) sapphire substrate, respectively. Next, (0001) ScAlN or (0001) MgZnO piezoelectric layer was epitaxially grown on epitaxial acoustic Bragg reflector, respectively. **Fig.1** shows cross sectional SEM images of epitaxial ScAlN SMR.

3. Crystal orientation

The crystal orientation of epitaxial thin films was determined by X-ray diffraction (X'Pert PRO, PANalytical). As shown in **Fig.2**, we can observe clear six symmetry in the $(10\bar{1}1)$ ScAlN pole figures of $Sc_{0.43}Al_{0.57}N$ SMR and $Sc_{0.20}Al_{0.80}N$ SMR. This indicates that epitaxial ScAlN piezoelectric layers on epitaxial acoustic Bragg reflector were fabricated.

4. Impedance characteristic

Impedance characteristic of full-epitaxial SMR was measured by a network analyzer (E5071C, Keysight Technologies). Resonance-antiresonance peak was observed around 1.8 GHz in the impedance characteristic of epitaxial $Sc_{0.43}Al_{0.57}N$ SMR based on 5 pairs of Ti/Pt (**Fig. 3(a)**). As shown in **Fig. 3(b)**, we can see resonance-antiresonance peak of epitaxial $Sc_{0.20}Al_{0.80}N$ SMR based on 6 pairs of ZnO/Pt around 2.1 GHz. Effective electromechanical coupling coefficient k_{eff}^2 of epitaxial $Sc_{0.43}Al_{0.57}N$ SMR and $Sc_{0.20}Al_{0.80}N$ SMR was determined to be 13.6% and 3.1% by resonance-antiresonance method[8)], respectively.

(a)

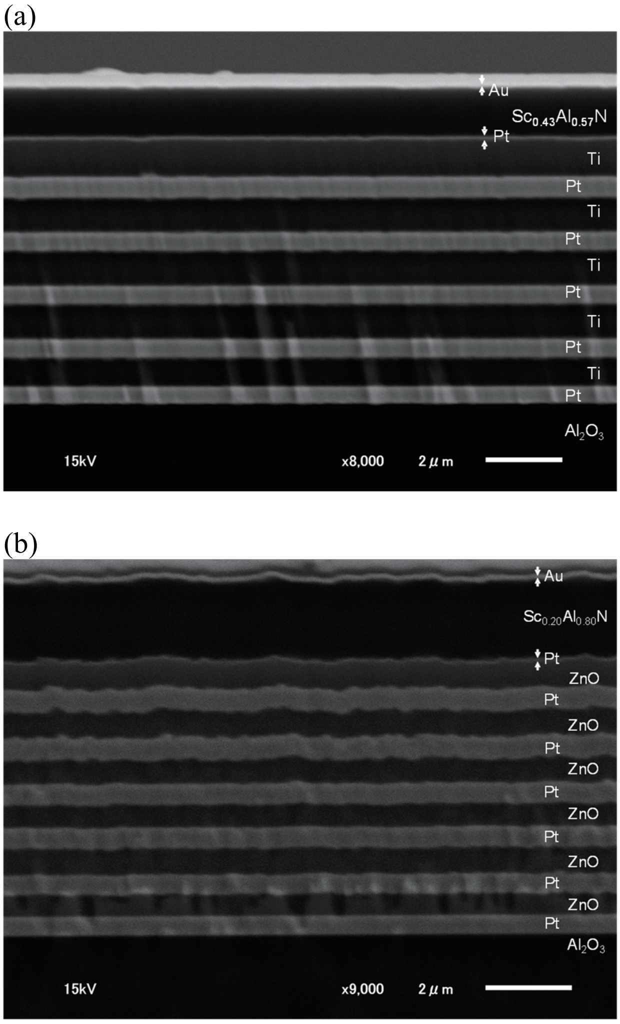

Fig. 1 Cross sectional SEM images of full-epitaxial SMR
(a) $Sc_{0.43}Al_{0.57}N$ SMR based on 5 pairs of Ti/Pt
(b) $Sc_{0.20}Al_{0.80}N$ SMR based on 6 pairs of ZnO/Pt

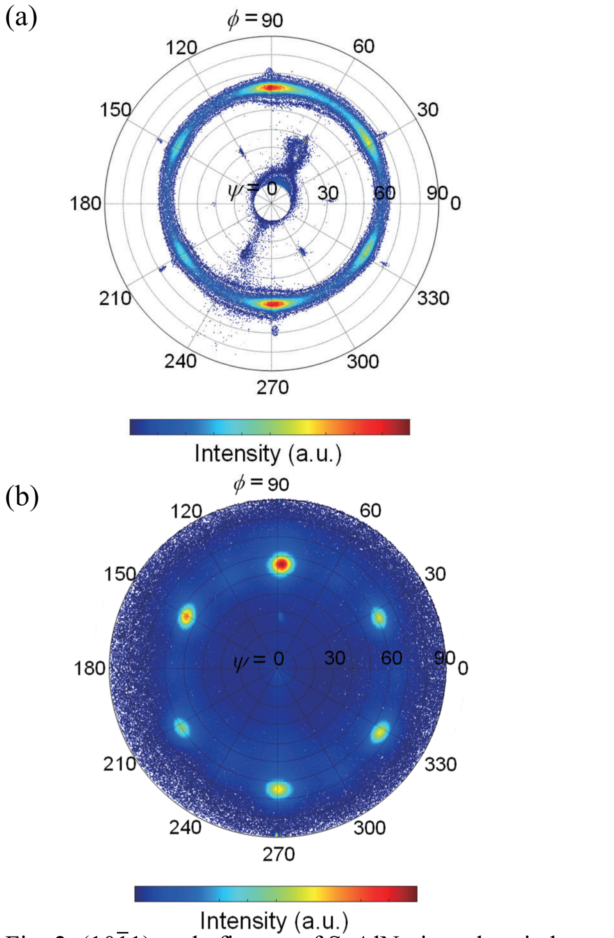

Fig. 2 $(10\bar{1}1)$ pole figures of ScAlN piezoelectric layer
(a) $Sc_{0.43}Al_{0.57}N$ SMR based on 5 pairs of Ti/Pt
(b) $Sc_{0.20}Al_{0.80}N$ SMR based on 6 pairs of ZnO/Pt

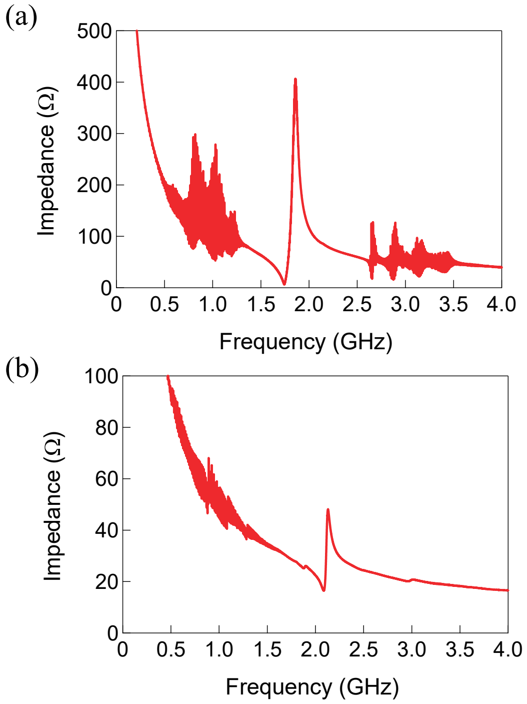

Fig. 3 Impedance characteristic of full-epitaxial SMR
(a) $Sc_{0.43}Al_{0.57}N$ SMR based on 5 pairs of Ti/Pt
(b) $Sc_{0.20}Al_{0.80}N$ SMR based on 6 pairs of ZnO/Pt

5. Conclusion

SMR with epitaxial ScAlN or MgZnO piezoelectric layer based on epitaxial Ti/Pt or ZnO/Pt acoustic Bragg reflector was characterized. Epitaxial ScAlN and MgZnO piezoelectric layers show good crystal orientation and clear six-fold symmetry. k_{eff}^2 of epitaxial $Sc_{0.43}Al_{0.57}N$ SMR and $Sc_{0.20}Al_{0.80}N$ SMR was determined to be 13.6% and 3.1% by resonance-antiresonance method, respectively.

Acknowledgment

This work was supported by JST-CREST (No. JPMJCR20Q1), JST-FOREST and KAKENHI (Grant-in-Aid for Scientific Research B, No.19H02202, No.21K18734).

References

1) L. Lv, Y. Shuai, X. Bai, S. Huang, D. Zhu, Y. Wang, J. Zhao, W. Luo, C. Wu and W. Zhang, IEEE Trans. Ultrason., Ferroelect., Freq. Contr. **69**, pp. 1535-1541 (2022).
2) A. Reinhardt, M. Bousquet, A. Joulie, C.-L. Hsu, F. Delaguillaumie, C. Maeder-Pachurka, G. Enyedi, P. Perreau, G. Castellan and J. Lugo, 2021 Joint Conference of the European Frequency and Time Forum and IEEE International Frequency Control Symposium (EFTF/IFCS), pp. 1-4 (2021).
3) Z. Fang, H. Jin, S. Dong, L. Lu, W. Xuan and J. Luo, Electronics Letters, pp 1142-1143 (2020).
4) M. Bousquet, P. Perreau, C. Maeder-Pachurka, A. Joulie, F. Delaguillaumie, J. Delprato, G. Enyedi, G. Castellan, C. Eleouet, T. Farjot, C. Billard and A. Reinhardt, Proc. IEEE Ultrason. Symp., no. 9251654 (2020).
5) X. Bai, Y. Shuai, L. LV, Y. Xing, J. Zhao, W. Luo, C. Wu, T. Yang and W. Zhang, J. Appl. Phys. **128**, no. 094503 (2020).
6) Y. Osugi, T. Yoshino, K. Suzuki and T. Hirai, IEEE/MTT-S Int. Microwave Symp., pp. 873-876 (2007).
7) K. M. Lakin, K. T. McCarron and R. E. Rose, Proc. IEEE Ultrason. Symp., (1995).
8) "IEEE Standard on Piezoelectricity (ANSI/IEEE Std 176-1987)," IEEE Ultrason., Ferroelect., and Freq. Contr. **43,** pp. 719-772, (1996).

E-mail:
†t.satoshi@akane.waseda.jp, *yanagitani@waseda.jp